PNAS
www.pnas.org

Supplementary Information for

Immunotherapy for breast cancer using EpCAM aptamer tumor-targeted gene knockdown

Ying Zhang, Xuemei Xie, Pourya Naderi Yeganeh, Dian-Jang Lee, David Valle-Garcia, Karla F. Meza-Sosa, Caroline Junqueira, Jiayu Su, Hongbo R. Luo, Winston Hide, Judy Lieberman

Judy Lieberman
Email: judy.lieberman@childrens.harvard.edu

This PDF file includes:

Supplementary text
Figures S1 to S7
Tables S1 and S2
SI References

Other supplementary materials for this manuscript include the following:

Datasets S1 and S2

Materials and Methods

Cell lines

L929 and P815 were obtained from ATCC. 4T1 were provided by Fred Miller (Wayne State University), N202.1A were provided by Paloma Giangrande (University of Iowa), B16-F10 were a gift of Gordon Freeman (Dana-Farber Cancer Institute) and EpCAM^{hi}MDA-MB-231 that were transduced with a lentiviral vector expressing human EpCAM were provided by Mark Cobbold (Massachusetts General Hospital). 4T1E was generated in our laboratory by sorting 4T1 cells for high E-cadherin expression. 4T1E-eGFP were generated using a pCAG-eGFP lentiviral vector. 4T1E stably expressing firefly luciferase (4T1E-Luc) were selected after infection with EF1a-Luciferase(firefly)-2A-RFP-Puro lentiviral vector (amsbio) using puromycin. Cell lines were cultured in DMEM supplemented with 10% heat-inactivated FBS (Gemini Bioproducts), 6 mM HEPES, 1.6 mM L-glutamine, 50 μM 2-mercaptoethanol, 100 U ml^{-1} penicillin G, and 100 μg ml^{-1} streptomycin sulfate (Sigma-Aldrich). All cell lines were verified to be free of mycoplasma by PCR and were authenticated by morphology.

Mouse studies

All animal experiments were conducted in compliance with all the ethical regulations and were approved by the Harvard Medical School Institutional Animal Care and Use Committee. All mice were housed in the Harvard Medical School Animal Facility. Female *BALB/c* mice (6-8 weeks old) were purchased from The Jackson Laboratories. *ErbB2ΔEx16*$^{+/-}$ transgenic mice and *MTB*$^{+/-}$ transgenic mice (harboring the MMTV/reverse tetracycline transactivator transgene) were kind gifts of William J. Muller (McGill University) (36). They were cross-bred to generate *ErbB2ΔEx16*$^{+/-}$*MTB*$^{+/-}$ double transgenic mice. Transgene expression was determined by genotyping for *ErbB2ΔEx16* (forward primer: 5'-GTGACCTGTTTTGGACCGGA-3', reverse primer: 5'-TCTCCGCATCGTGTACTTCC-3') and *MTB* (forward primer: 5'-ACCGTACTCGTCAATTCCAAGGG-3', reverse primer: 5'-TGCCGCCATTATTACGACAAGC-3'). 8-week-old female *ErbB2ΔEx16*$^{+/-}$*MTB*$^{+/-}$ mice were given 2 mg/ml doxycycline (Sigma-Aldrich) in the drinking water throughout the study. Mice treated with doxycycline for three days were randomly assigned to either control or treatment groups and were treated with the EpCAM-AsiC cocktail (5 mg/kg in PBS for each AsiC; total 30 mg/kg) or EpCAM aptamer (30 mg/kg) every third day. Tumor onset was monitored by palpation and tumor growth was assessed by measuring the perpendicular diameters of tumors every other day. The mice were euthanized on day 28.

For orthotopic tumor challenge, 4T1E (~10^5 cells/mouse) or 4T1E-eGFP (~$3x10^5$ cells/mouse) were injected into the 4th mammary fat pad of *BALB/c* mice. When tumors became palpable (approximately 3-4 days post tumor challenge), mice were injected subcutaneously with PBS (mock), 5 mg/kg of EpCAM aptamer or 5 mg/kg of individual EpCAM-AsiC every third day. Tumor growth was monitored by measuring the perpendicular diameters of tumors daily. When the average diameter of control group tumors reached ~4-5 mm (around two weeks), all mice in an experiment were euthanized and tumors were collected for analysis. In Figure 1B, to determine the longer-term anti-tumor efficacy of UPF2 EpCAM-AsiC, mice were challenged with $5x10^4$ 4T1E and the

treatment was initiated on day 8 post tumor challenge. Tumor growth was monitored for 25 days. For cell depletion, CD8 antibody (clone 2.43), CD4 antibody (clone GK1.5), CSF1R antibody (clone AFS98) or the isotype control antibody (all from BioXCell) were injected intraperitoneally (i.p., 300 μg/mouse) into mice bearing 4T1E tumors. CD8 or CD4 antibody was given starting on day 2 after tumor challenge for three consecutive days, and every five days thereafter. Anti-CSF1R was injected starting on day 2 after tumor challenge and every other day afterwards. Immune cell depletion was verified by flow cytometry using peripheral blood mononuclear cells obtained on day 7 after tumor challenge and/or tumor-infiltrating immune cells obtained at necropsy. For anti-CD47 (clone MIAP301, BioXcell) treatment, the antibody was injected i.p. (400 μg/mouse) starting on day 3 of tumor challenge and every third day thereafter. The PARP1 inhibitor olaparib (LC Laboratories) was dissolved in DMSO to 50 mg/ml and then diluted with 10% 2-hydroxyl-propyl-β-cyclodextrin/PBS (Sigma-Aldrich), and 50 mg/kg was given to mice daily i.p. starting on day 3 after tumor challenge for a total of 12 injections. Anti-PD-1 (200 μg/mouse, clone 29F.1A12, BioXCell) was administered when indicated starting on day 10 after tumor challenge and every third day thereafter.

To assess the anti-tumor efficacy of EpCAM-AsiC against lung metastatic breast tumors, 4T1E-Luc were first mixed with 150 μg/ml of D-luciferin (PerkinElmer) and their luciferase activity was checked by luminescent imaging using the IVIS Lumina II system (Caliper Life Sciences). *BALB/c* mice were injected intravenously with 4T1E-Luc ($3x10^5$ cells/mouse) and treated with either EpCAM aptamer or the EpCAM-AsiC cocktail starting on day 7 post tumor challenge. After i.p. injection of 150 mg/kg of D-luciferin, whole body luminescent images were taken immediately after tumor challenge and every 5 days thereafter for 20 days. The lungs were isolated at necropsy for analysis.

RNAs

The 19 nt EpCAM aptamer (8) with 2'-fluoropyrimidines was used as control RNA. Candidate mouse or human gene-specific, or mouse and human gene cross-reactive siRNAs were either predesigned ON-TARGETplus siRNAs and/or designed using the siDESIGN tool (both from Dharmacon). siRNAs used to construct EpCAM-AsiC were selected based on their gene knockdown *in vitro* in mouse and/or human breast cancer cell lines, as measured by qRT-PCR. ON-TARGETplus non-targeting pool siRNAs were used as negative control. siRNA sequences with the most gene knockdown efficiency and lowest Tm values were selected. For EpCAM aptamer-siRNA conjugation, the long strand of the AsiC, designed by linking the EpCAM aptamer to the sense strand of the siRNA via a U-U-U linker, was synthesized with 2'-fluoropyrimidine substitutions and a 3'-dTdT overhang and annealed to the antisense strand of the siRNA, which was also modified with a 3'-dTdT overhang, using a 2-fold molar excess of the short strand. The long strand RNA oligo was initially heated to 95 °C for 10 min. Then the short strand RNA was added to anneal with the long strand at 65 °C for 7 min. The mixture was allowed to cool at room temperature for 20 min. The annealed EpCAM-AsiC duplexes were purified further using Illustra MicroSpin G-25 columns. EpCAM-AsiC sequences are provided in Table. S1.

Gene knockdown and qRT-PCR

To measure *in vitro* siRNA-mediated gene silencing, cells were seeded (10^4 cells/well) in 96-well plates and transfected with siRNAs ranging from 6.25 nmol/L to 100 nmol/L using Dharmafect I according to the manufacturer's protocol. Cells were transfected in serum- and antibiotic-free medium for 6-8 h before adding culture medium supplemented with 20% FBS. RNA was extracted 24-48 h later and gene knockdown was assessed by qRT-PCR. To measure *in vitro* EpCAM-AsiC-mediated gene silencing, cells were incubated with 4 μmol/L of EpCAM aptamer or EpCAM-AsiC in WIT-T medium. Gene knockdown was assessed by measuring mRNA and protein 72-96 h after treatment by qRT-PCR and flow cytometry, respectively. Cell viability was measured by CellTiter-Glo 24-72 h after treatment as indicated. Cell proliferation was measured by CellTiter 96 A_{queous} One Solution Cell Proliferation assay (MTS assay). To assess *in vivo* gene silencing, tumors were collected from mice treated with EpCAM aptamer or EpCAM-AsiC. Single cell suspension was prepared by tumor digestion and homogenization. Dead cells were removed and $CD45^-EpCAM^+$ tumor cells were enriched by negative selection using CD45 microbeads and positive selection using CD326 (EpCAM) microbeads according to the manufacturer's protocol. $CD45^-EpCAM^-$ cells from the same tumors were collected as control. Gene knockdown in each cell subset was measured by qRT-PCR and flow cytometry. For qRT-PCR, total RNA was extracted with TRIzol and Direct-zol RNA miniprep kit and RNA concentrations were quantified with a NanoDrop 2000 Spectrophotometer. cDNA synthesis was performed using the High Capacity cDNA Reverse Transcription kit. qRT-PCR of cDNAs was performed with primers corresponding to the target genes or housekeeping gene *Gapdh* (IDT) (Table. S2), SsoFast EvaGreen Supermix and Bio-Rad C1000 Thermal Cycler.

Histology and IHC

Tumors were fixed with 10% formalin, stored in 70% ethanol, and embedded in paraffin. Sections (5 μm) were cut, air-dried, fixed for hematoxylin and eosin (H&E) staining and IHC staining by the Dana-Farber Cancer Institute Rodent Histopathology Core and Dana-Farber/Harvard Cancer Center Specialized Histopathology Core as previously described (1). Anti-CD8 (clone 4SM15, ThermoFisher) was used at 5 μg/ml. The slides were scanned into the Aperio image analysis platform. The numbers of $CD8^+$ T cells were then visualized and digitally annotated in regions of interest (5 fields/slide) using ImageScope software and analyzed using image analysis algorithms (Aperio Technology).

Isolation of immune cells from mice

Peripheral blood mononuclear cells and tumor-infiltrating cells (TIC) were collected as described (2). Briefly, blood was collected by submandibular puncture and PBMCs were isolated by Histopaque gradient centrifugation. Red blood cells were lysed with 1x RBC lysis buffer. To isolate TIC, tumors were cut into small pieces and treated with digestion buffer (RPMI supplemented with 2 mg/ml collagenase D, 100 μg/ml DNase I and 2% FBS) with agitation for 30 min at 37 °C. Samples were then homogenized and filtered through 40 μm strainers, and immune cells were purified by Percoll gradient centrifugation and washed with Leibovitz's L-15 medium.

Antibody staining and flow cytometry

Immune cells or tumor cells isolated from mice were stained with anti-CD45-PerCPCy5.5 or -PacBlue, CD3-PE-Cy7, -FITC or APC, CD8-PacBlue, -PerCPCy5.5, -Alexa700, -FITC or -APC, CD4-PE-Cy7, -APC or PerCPCy5.5, CD19-FITC, CD25-PE, CD44-PerCPCy5.5 or PacBlue, Ly-6G/Ly-6C(Gr-1)-FITC or -PE, CD11b-Alexa700, CD11c-APC or PE-Cy7, DEC205-PE, CD49b-PacBlue or FITC, NKp46-APC, F4/80-PE-Cy7, I-A/I-E(MHCII)-PacBlue, CD206-APC, TCR-β-FITC, TER-119-FITC, EpCAM-PE-Cy7 or PerCPCy5.5, CD47-FITC, CD274-APC, CD40-APC, CD86-FITC, CD107a-APC, CD107b-Alexa647, PD-1-PE-Cy7, 2B4-FITC, CTLA-4-PE, LAG-3-APC, TIM-3-PerCPCy5.5, H2A.X-phosphorylated (Ser139)-APC. Dead cells were excluded using the live/dead fixable aqua dead cell stain added with cell-surface antibodies. Mouse TAMs were defined as live$^+$CD45$^+$CD3$^-$CD19$^-$Ter119$^-$TCRβ$^-$CD11b$^+$F4/80$^+$. M1 TAMs were defined as live$^+$CD45$^+$CD3$^-$CD19$^-$Ter119$^-$TCRβ$^-$CD11b$^+$F4/80$^+$CD206$^-$MHCII$^+$ and M2 TAM were defined as live$^+$CD45$^+$CD3$^-$CD19$^-$Ter119$^-$TCRβ$^-$CD11b$^+$F4/80$^+$CD206$^+$MHCII$^+$. (TAM that did not meet either of these criteria were not classified.) For intracellular staining of GzmB or PFN, cells were first stained with antibodies to cell-surface markers for 30 min at 4 °C, then fixed and permeabilized with fixation/permeabilization buffer and stained with anti-GzmB-PacBlue, and Perforin-PE. For staining of Foxp3, UPF2, or γH2A.X, cells were first stained for surface markers, then fixed and permeabilized with Foxp3/Transcription factor staining buffer set and stained with Foxp3-PercpCy5.5 or PE, primary antibody against UPF2 or rabbit monoclonal IgG Isotype antibody, or γH2A.X-APC. UPF2 was further detected with goat anti-rabbit IgG H&L-APC secondary antibody. For TUNEL staining, single cell suspensions of tumor samples were stained for surface antigens and fixed and permeabilized with Foxp3/Transcription factor staining buffer. TUNEL+ tumor cells were analyzed with APO-BrdU TUNEL Assay Kit. For intracellular cytokine staining of *ex vivo* stimulated lymphocytes, ~10^6 cells per sample were cultured in RPMI medium containing 2% FBS and were stimulated with PMA (50 ng/ml), ionomycin (2 μg/ml) and Golgiplug (1.5 μg/ml) for 4 h. Cells cultured with medium and Golgiplug alone served as negative control. Cells were then stained with antibodies to IFN-γ-PacBlue or -APC and TNF-α-PE-Cy7 after fixation/permeabilization. Cells were analyzed by BD FACSCanto II and data were analyzed with FlowJo V.10.

CD8$^+$ TIL degranulation and cytotoxicity assay

Single-cell suspensions of TIC were enriched for CD45$^+$ or CD8$^+$ cells using CD45 or CD8 microbeads, respectively (Miltenyi Biotec). For degranulation assay, the number of CD8$^+$ TIL in freshly isolated CD45$^+$ cells was first determined by flow cytometry. CD8$^+$ TIL were co-incubated with autologous target tumor cells plated one day earlier in 48-well plates at a ratio of 1:3 in RPMI medium containing 10% FBS. Antibodies to CD107a-APC and CD107b-APC (each 1 mg/ml) and IL-2 (100 IU/ml) were added at the start of the co-culture. Positive control cells were treated with PMA (50 ng/ml) and ionomycin (2 μg/ml) while negative control samples were treated with medium and IL-2. The co-culture was incubated for 1 h at 37°C in a 5% CO2 incubator, followed by the addition of the secretion inhibitors monensin (1:1000) and Golgi Plug (1.5 μg/ml) for an additional 5 h. TIL were removed from the co-culture and re-plated in 96-well plates after stimulation and were stained for live cells and then with antibodies to CD8, IFN-γ, and TNF-α after fixation/permeabilization. For CD8$^+$ TIL cytotoxicity assay, autologous tumor cells were

labeled with ^{51}Cr and plated one day earlier in 96-well plates. Freshly isolated $CD8^+$ TIL were co-cultured with tumor cells at a ratio of 5:1 in RPMI containing 10% FBS and IL-2 (100 IU/ml) for 30 h. Maximal ^{51}Cr release was determined by adding 1% SDS and spontaneous ^{51}Cr release was measured using $CD8^+$ TIL cultured in medium and IL-2 alone. The percentage of target cell lysis was calculated using the formula: % specific lysis=((test ^{51}Cr release) – (spontaneous ^{51}Cr release)) / ((maximal ^{51}Cr release) − (spontaneous ^{51}Cr release)) x100.

***Ex vivo* phagocytosis assay**

Dead cells were removed using a dead cell removal kit and TAM were enriched from tumor-infiltrating immune cells using F4/80 microbeads. The number of $live^+CD11b^+F4/80^+$ TAM in freshly isolated $F4/80^+$ cells was first determined by flow cytometry. 4T1E-eGFP tumors were either treated with negative control or CD47 siRNA 72 h earlier to knockdown *Cd47*. 50,000 TAMs were co-cultured with 200,000 4T1E-eGFP cells in RPMI serum-free medium for 3 h at 37°C and then washed three times with DPBS supplemented with 0.5% BSA and 2 mM EDTA, stained with anti-CD45, CD11b, and F4/80 and analyzed by flow cytometry. TAM that were GFP high were counted as phagocytic.

Single-cell RNA sequencing

Sample preparation

BALB/c mice were orthotopically implanted with ~10^5 4T1E cells/mouse. Three days post tumor challenge mice were treated with either EpCAM aptamer or EpCAM-AsiC cocktail targeting *Upf2, Parp1, Cd47* and *Mcl1* by s.c. injection every third day. On day 14, tumors were harvested, incubated at 37°C for 15 min with 100 μg/ml Liberase TL diluted in Ca^{2+} and Mg^{2+}-free RPMI, followed by shaking at 37°C for 10 min. Samples were then filtered twice through 40 μM strainers. Dead cells were removed and $CD45^+$ cells were enriched with CD45 microbeads at 4°C. More than 95% of cells were $CD45^+$ as verified by flow cytometry. The enriched cells were diluted to 2x10^5 cells/ml in Ca^{2+} and Mg^{2+}-free RPMI medium containing 1% FBS and kept on ice until the cells were flowed into the microfluidic device. 6,000 cells per sample were encapsulated using the inDrop technology (3), with half of the samples used for library preparation and the other half stored for backup. Two biological replicates per condition were processed independently and sequencing data from both samples were combined for data analysis. Single-cell encapsulation and RNA capture on the inDrop platform as well as library preparation were performed at the Harvard Medical School Single Cell Core. Single-cell transcriptomes were barcoded within the microfluidic droplets. After within droplet reverse transcription, emulsions of approximately 3,000 cells were broken and used for library preparation. Libraries were indexed with V3 sequencing adaptors, pooled from different samples at equimolar ratios, and sequenced on an Illumina NextSeq 500 system using the NextSeq 75 High Output Kits and standard Illumina sequencing primers and 61 cycles for read 1 and 14 cycles for read 2, 8 cycles each for index read 1 and index read 2.

Data Processing

Raw data were processed using the InDrops pipeline in Python (https://github.com/indrops/indrops) for version 3 libraries with default parameters (3). Briefly, reads were filtered by the quality and separated by corresponding library indexes. Valid reads were then demultiplexed and sorted by cell barcodes. Cell barcodes containing fewer than 250 total reads were discarded, and remaining reads were aligned to a reference mouse transcriptome (Ensembl GRCm38 release 85). Aligned reads were then quantified as an UMI-filtered mapped (UMIFM) count matrix that was used for all downstream analyses.

Pre-clustering filtering, normalization and batch correction

Analysis of the processed data was performed in R version 3.5.2 using the Seurat package version 2.3. All samples were merged. The percentage of mitochondrial transcripts for each cell (percent.mito) and average UMI of each gene (nUMI.nGene.ratio) were calculated. Low-quality cells were filtered using the following cutoffs: nGene —min. 50, max. 2000; percent.mito —min. -Inf, max. 0.25; nUMI.nGene.ratio —min. 1, max 5. The NormalizeData function was performed using default parameters to remove the differences in sequencing depth across cells. The ScaleData function was used to eliminate cell-cell variation in gene expression driven by batch and mitochondrial gene expression.

Dimension reduction and unsupervised clustering

Dimension reduction was performed at three stages of the analysis: the selection of variable genes, PCA, and uniform manifold approximation and projection (UMAP). The FindVariableGenes function was applied to select highly 2274 variable genes covering most biological information contained in the whole transcriptome. Then, the variable genes were used for PCA implemented with the RunPCA function. Next, we selected PCs 1-20 as input to perform the RunUMAP function to obtain bidimensional coordinates for each cell. We performed the FindClusters function (resolution 0.4) to cluster cells using the Louvain algorithm based on the same PCs as RunUMAP function.

Identification of DEGs and GO analysis

The FindMarkers or FindAllMarkers function (test.use = ‘‘t’’, logfc.threshold = log(1.6)) based on normalized data was used to identify differentially expressed genes (DEGs). P-value adjustment was performed using Bonferroni correction based on the total number of genes in the dataset. DEGs with adjusted p-values>0.05 were filtered out. Gene ontology (GO) analysis was performed by using the R package clusterProfiler.

Bulk RNA sequencing

EpCAM^{hi}MDA-MB-231 cells were transfected with 100 nM of negative control siRNA or ON-TARGETplus human UPF2 siRNA-SMARTpool for 72 h. The transfection

achieved >80% *UPF2* mRNA knockdown. Total RNA was extracted from each sample using TRIzol and Direct-zol RNA miniprep kit. Three biological replicates per condition were used for RNA-sequencing library preparations. The RNA integrity number (RIN) of all samples was determined by an Agilent 2100 Bioanalyzer in the Harvard Medical School Biopolymers Facility. All RNA samples had RINs greater than 9. Standard mRNA libraries were prepared with NEBNext® Ultra™ II Directional RNA Library Prep Kit after polyA-mRNA isolation (New England BioLabs). Libraries for negative control and *UPF2* siRNA transfected samples were pooled separately and each pool was run on one lane of an Illumina Hiseq X10 PE100 system, yielding around 240 million mapped 150 bp paired-end reads per sample. Sequences were aligned against reference genome GRCh38 (Ensembl release 98) using HISAT2. A pipeline incorporating DEXSeq and HTSeq counts was used to identify differential exon usage (DEU) events using the reference GRCh38_98. The DEU analysis was limited to exons with at least 10 reads in at least 3 samples. DEU events were significant if they reached a multiple-hypothesis adjusted p-value < 0.05. StringTie was used to assemble reads into novel and annotated transcripts using the guided-assembly approach on the GRCh38_98 reference. Per-sample assemblies were then integrated into a unified transcript reference using StringTie's merge functionality. Kallisto was used to quantify transcript abundance from the StringTie-generated reference. Differential isoform usage events (DIU) were identified with IsoformSwitchAnalyzer. IsoformSwitchAnalyzer also provided predictions of premature termination codons (PTC), for readout of potential NMD sensitivity. Changes in isoform usage were significant if they reached a q-value < 0.05.

Statistical analysis

A Student's t-test (two-tailed) or Mann-Whitney test was used to determine differences between two groups. One- or two-way ANOVA, or Kruskal-Wallis test was used to calculate differences among multiple populations. Differences between tumor growth curves were compared by first calculating the area-under-curve values for each sample and then comparing different groups using the Student's t-test or one-way ANOVA. Comparisons of tumor volumes at different time points along tumor growth were determined by multiple t-test with type I error correction. Type I errors were corrected by the Holm-Sidak or Dunn's multiple comparisons test. Nonparametric test was used when data did not follow a normal distribution. Significance was set at p-value ≤ 0.05. For all figures, *, $p \leq 0.05$, **, $p \leq 0.01$, ***, $p \leq 0.001$, ****, $p \leq 0.0001$. All statistical analyses were conducted using GraphPad Prism 8.

Fig. S1

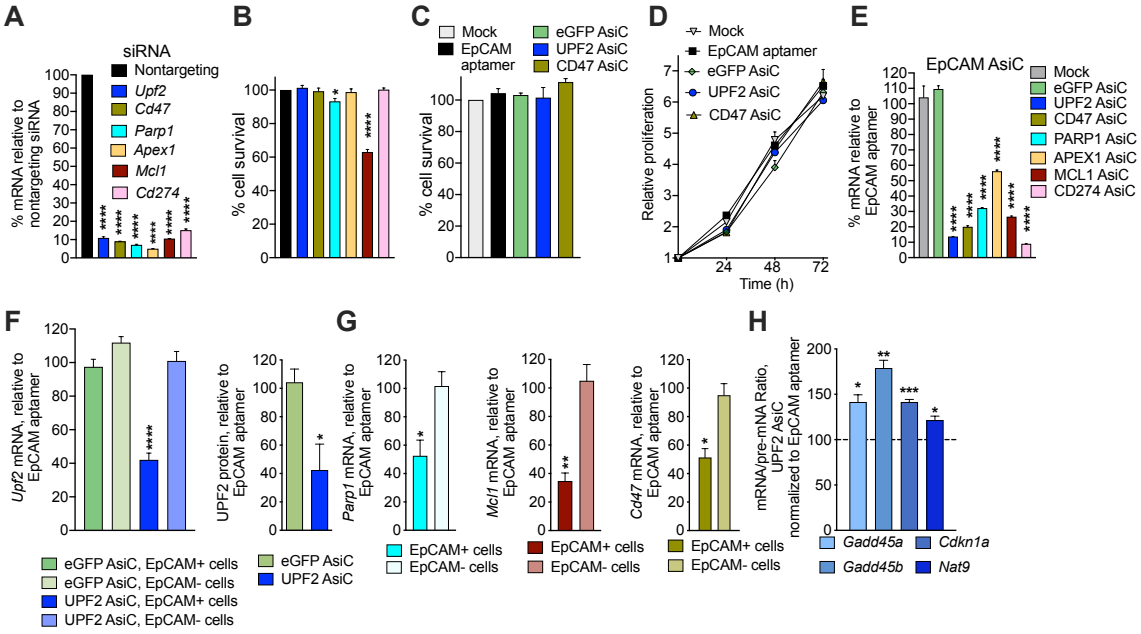

Fig. S1. EpCAM-AsiCs-mediated gene knockdown in EpCAM+ 4T1E. (A-B) Gene knockdown (A) and cell viability by CellTiter-Glo assay (B) of 4T1E, assessed 72 h after in vitro transfection of 100 nM siRNA and normalized to control cells transfected with nontargeting siRNA (n=3-5). **(C-D)** Cell viability (C) and proliferation by MTS assay (D) of 4T1E treated with medium (mock) or 4 mM EpCAM aptamer or EpCAM-AsiCs targeting Upf2 or Cd47 for 72 h (n= 4). **(E)** Target gene mRNA assessed by qRT-PCR 72 h after incubation with 4 µM EpCAM-AsiCs and normalized to expression in cells treated with EpCAM aptamer (n=3). Upf2 mRNA expression in mock and eGFP AsiC treated cells relative to EpCAM aptamer treated cells were shown. **(F)** In vivo Upf2 mRNA (left) and protein (right) in CD45$^-$EpCAM$^+$ 4T1E and CD45$^-$EpCAM$^-$ cells isolated from 4T1E tumors treated with EpCAM aptamer, eGFP AsiC or UPF2 AsiC. **(G)** Parp1, Mcl1, and Cd47 mRNA in EpCAM$^+$ 4T1E tumor cells and CD45$^-$EpCAM$^-$ cells isolated from 4T1E tumors in mice treated with EpCAM aptamer or EpCAM-AsiC specific for the measured mRNA (n=3). **(H)** mRNA/pre-mRNA ratio of known NMD-targeted transcripts in EpCAM+ tumor cells isolated from mice treated with UPF2 AsiC normalized to those from mice treated with EpCAM aptamer (n=3). Data shown are mean + s.e.m. and represent at least two independent experiments. Statistical tests: A-C and E, One-way ANOVA with Holm-Sidak's multiple comparisons. D, Two-way ANOVA with Holm-Sidak's multiple comparisons. H, Multiple t-test with Holm-Sidak's multiple comparisons. *p ≤ 0.05, **p ≤0.01, ***p ≤0.001, ****p ≤0.0001.

Fig. S2

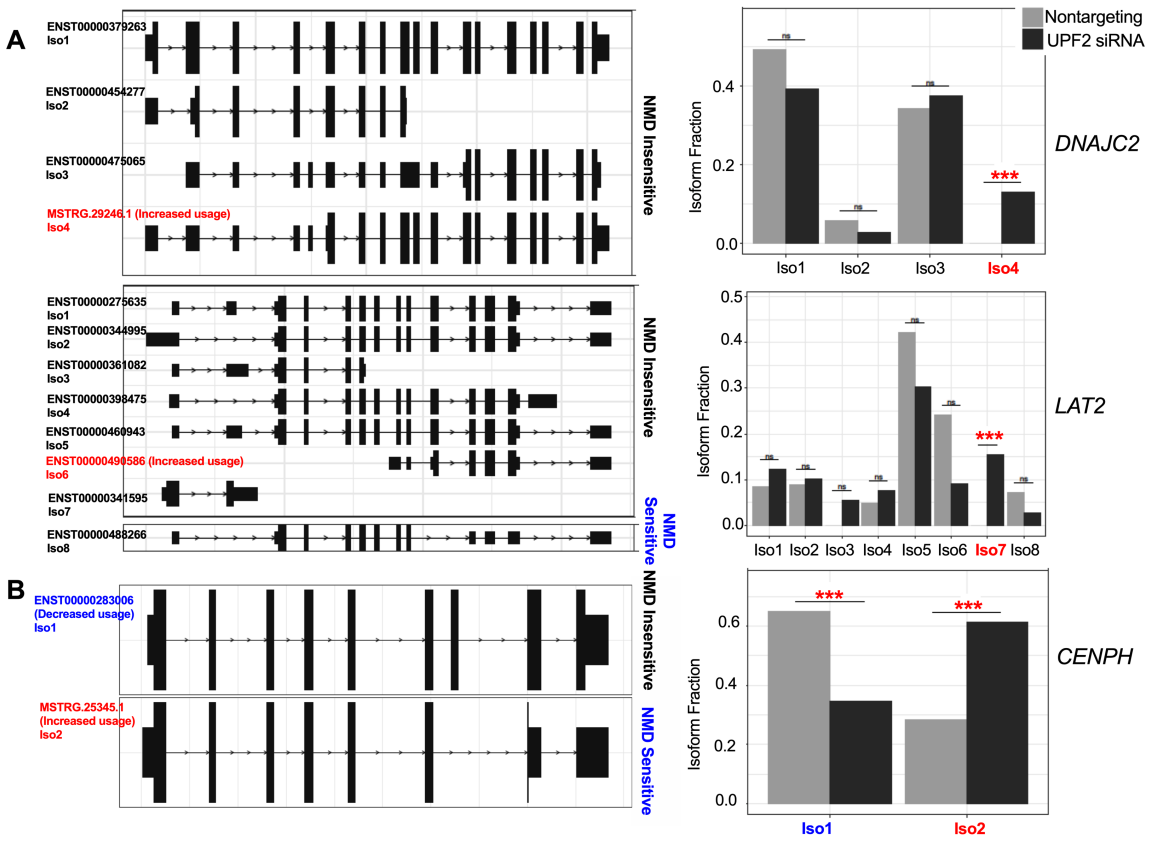

Fig. S2. *UPF2* knockdown in MDA-MB-231 generates novel mRNA isoforms and increases NMD-sensitive isoforms. (A) mRNA isoforms (NMD insensitive and sensitive transcripts indicated on right) of *DNAJC2* (upper) and *LAT2* (lower) (left). Proportion of the indicated isoforms sequenced in RNA-seq analysis of tumor cells transfected with nontargeting siRNA (grey) or UPF2 siRNA (black) (right). **(B)** mRNA isoforms (one protein coding NMD-insensitive transcript and one NMD sensitive transcript) of *CENPH* (left). Proportion of each isoform in tumor cells transfected with nontargeting siRNA (grey) or UPF2 siRNA (black) (right). In the left diagrams, longer black bars indicate protein-coding exons; shorter black bars indicate non-coding exons; lines in between represent introns. *q<0.05 and ***q<0.001. Higher q-values annotated as 'ns'. The DIU events were detected using the isoformSwitchTestDEXSeq.

Fig. S3

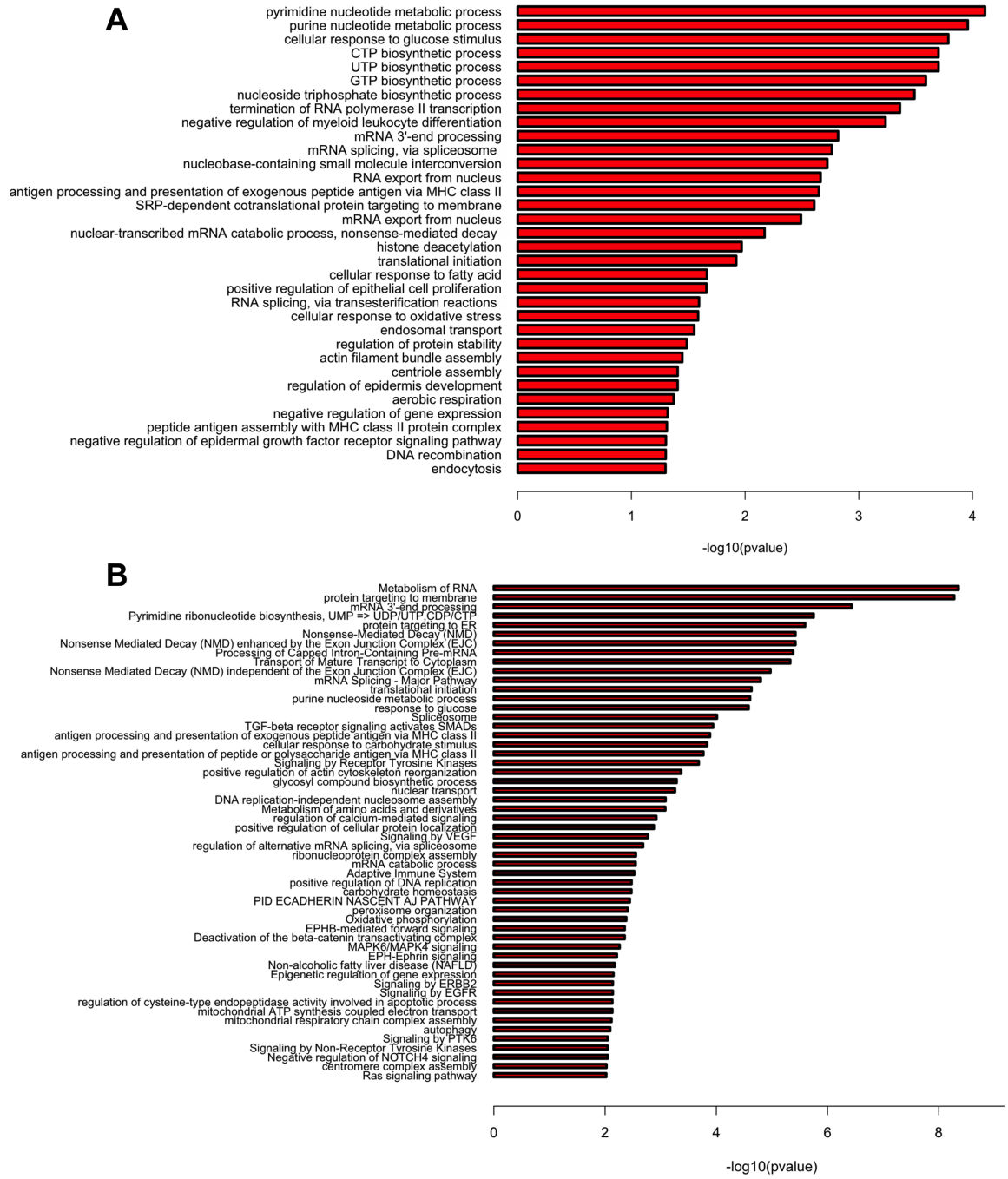

Fig. S3. Gene ontology analyses of pathways enriched in DEU genes generated in MDA-MB-231 cells knocked down of *UPF2*. Enriched terms analyzed by David **(A)** and Metascape **(B)** are shown.

Fig. S4

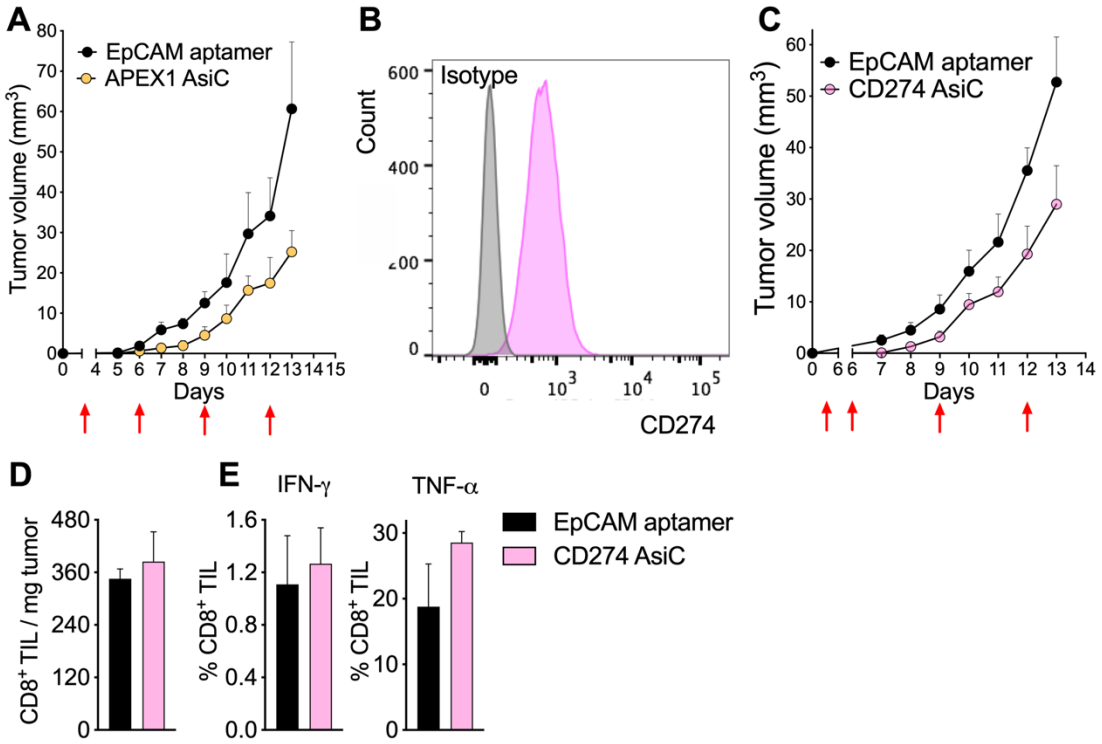

Fig. S4. 4T1E tumor inhibition and immune modulation after treatment with CD274 AsiC targeting PD- L1. (A) Growth of 4T1E orthotopic tumors in mice treated beginning on day 3 with EpCAM aptamer or APEX1 EpCAM-AsiC (5 mg/kg, every 3rd day) (n=5). **(B)** Flow cytometry histogram of PD-L1 expression on 4T1E tumor cells isolated from tumor-bearing mice. Cells were gated on live$^+$CD45$^-$EpCAM$^+$ cells. **(C)** 4T1E tumor growth in mice treated with EpCAM aptamer or CD274 AsiC (red arrows). **(D-E)** Flow cytometry analysis of single cell suspensions isolated on day 13 after tumor implantation from mice treated with EpCAM aptamer or PD-L1 AsiC for numbers of CD8$^+$ TIL per mg tumor (D) or percentages of CD8$^+$ TIL producing IFN-γ and TNF-α after stimulation with PMA and ionomycin (E). (C-E, n=5). Data shown are mean + s.e.m. Statistical test: A and C, tumor growth curves were compared by calculating the area under the curve values for each sample followed by Student's t-test. D-E, Student's t-test.

Fig.S5

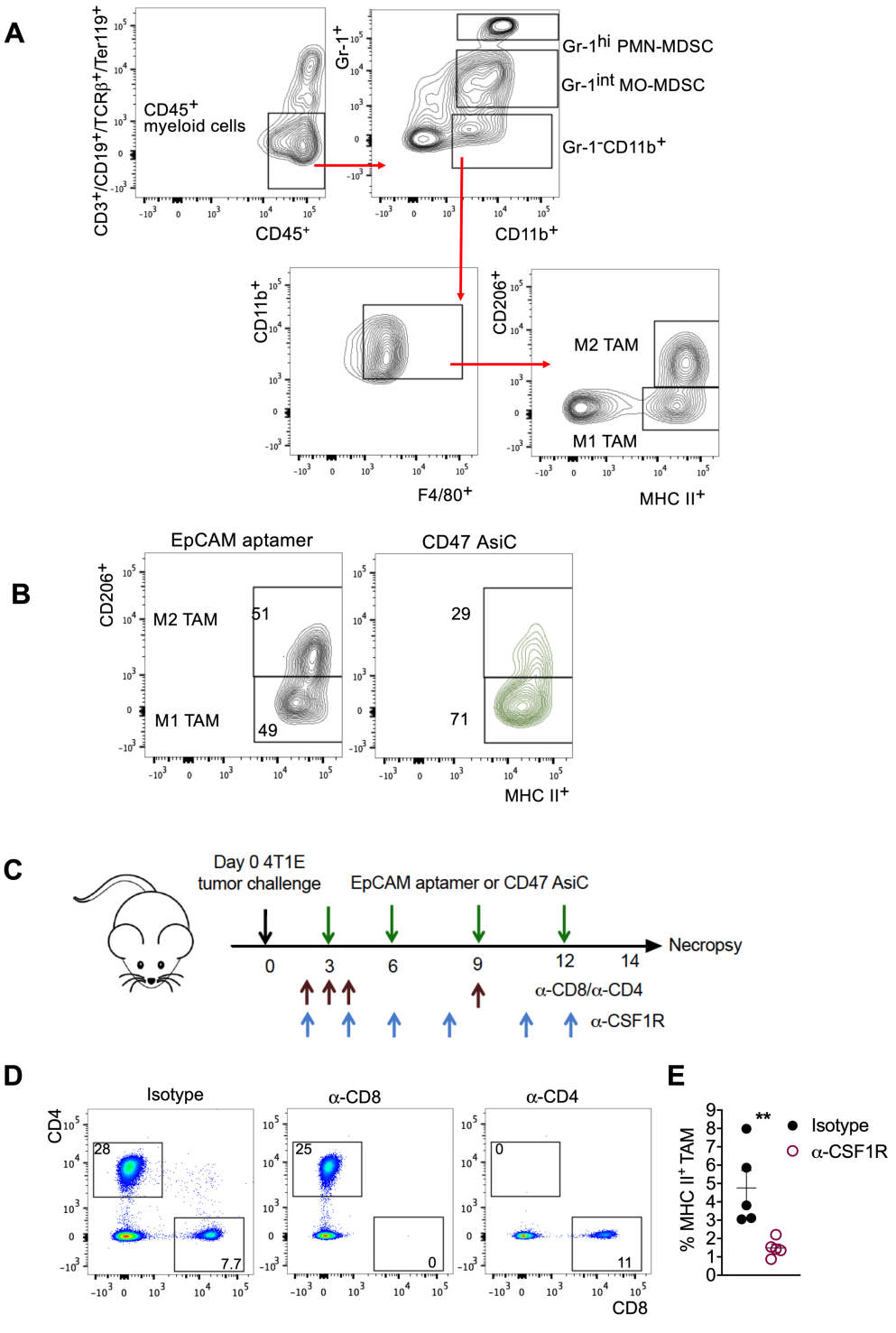

Fig. S5. CD47 AsiCs inhibit tumor growth by enhancing anti-tumor immunity. (A) Mononuclear, singlet, live tumor-infiltrating immune cells were first gated on $CD45^+$ cells,

gating out $CD3^+/CD19^+/TCR\beta^+/Ter119^+$ cells. The remaining $CD45^+$ myeloid cells were gated for Gr-$1^{hi}CD11b^+$ PMN-MDSCs, Gr-$1^{int}CD11b^+$ MO-MDSCs and Gr-1^- $CD11b^+$ cells. The Gr-1^-CD11b^+ cells were then gated for $F4/80^+$ TAMs and $CD206^-MHCII^+$ M1-like TAMs and $CD206^+MHCII^+$ M2-like TAMs. **(B)** Comparison of M1 to M2 TAMs in EpCAM aptamer or CD47 AsiC treated 4T1E tumors. Cells were gated on $CD45^+CD11b^+F4/80^+MCHII^+$ TAM. Numbers indicate percentages of each subset within $MHCII^+$ TAM. **(C)** Experimental scheme of CD47 AsiC treatment and immune cell depletion in mice bearing 4T1E tumors. **(D)** Representative flow plots of $CD4^+$ and $CD8^+$ T cells in peripheral blood of mice treated with isotype control Ab or anti-CD8 or anti-CD4. **(E)** Percentage of $CD11b^+F4/80^+MHCII^+$ TAM in $CD45^+$ tumor- infiltrating immune cells in mice treated with isotype control or anti-CSF1R. (n=5). Data shown are mean +/- s.e.m. Statistical test: E, Student's t-test. $^{**}p \leq 0.01$.

Fig. S6

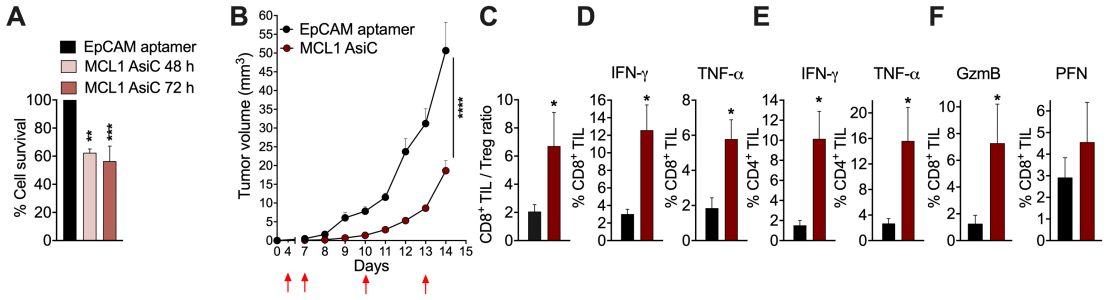

Fig. S6. Tumor inhibition and immune modulation after treatment with MCL1 AsiC. (A) Viability of 4T1E treated *in vitro* with 4 μM MCL1 EpCAM-AsiC for 48 and 72 h, relative to cells treated with 4 μM EpCAM aptamer. **(B)** Tumor growth in mice treated with EpCAM aptamer or MCL1 AsiC. Red arrows indicate each treatment. **(C-F)** Flow cytometry analysis of TIL isolated on day 14 after tumor implantation from mice treated as in (B). **(C)** $CD8^+/CD4^+Foxp3^+$ Treg ratio. **(D-E)** Percentage of $CD8^+$ (D) and $CD4^+$ (E) TIL producing IFN-γ and TNF-α after stimulation with PMA and ionomycin. **(F)** GzmB and PFN staining of $CD8^+$ TIL. Data shown are mean + s.e.m. and are representative of two experiments. For all panels, n=5. Data shown are mean + s.e.m. Statistical test: A, one-way ANOVA with Holm-Sidak's multiple comparisons. B, tumor growth curves were compared by calculating the area under the curve values for each sample followed by Student's t-test. C-E, Student's t-test. F, Mann-Whitney test. *$p \leq 0.05$, **$p \leq 0.01$, ***$p \leq 0.001$, ****$p \leq 0.0001$.

Fig. S7

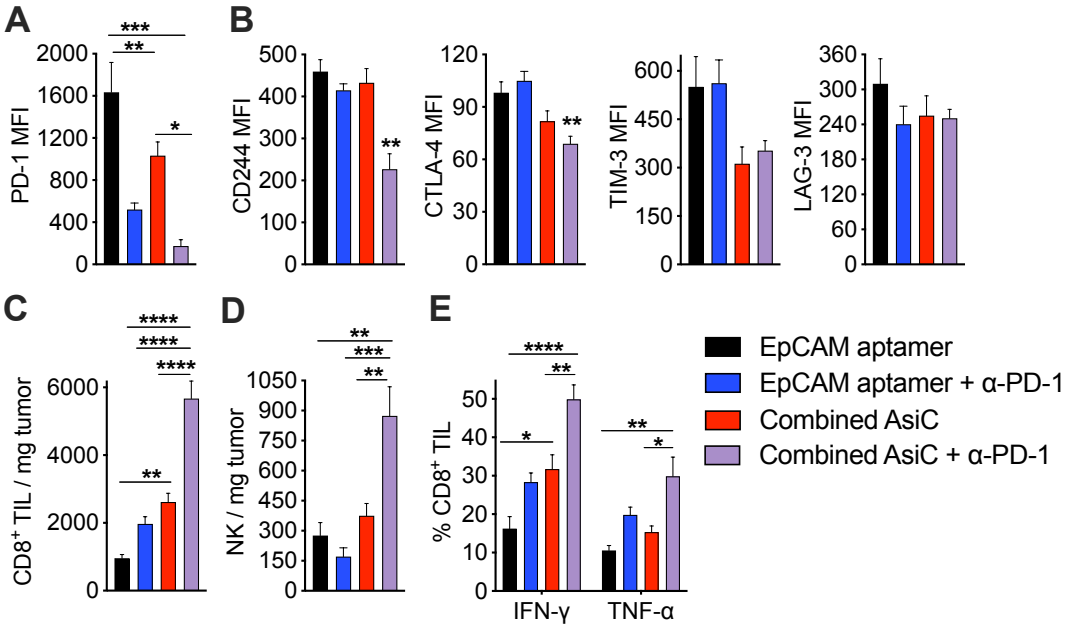

Fig. S7. Improved anti-tumor immunity by combining immune-modulating EpCAM-AsiCs with anti-PD-1. TIL, isolated on day 18 after tumor implantation from 4T1E orthotopic tumor-bearing mice treated with EpCAM aptamer, anti-PD-1 Ab, or a cocktail of AsiCs targeting *Upf2, Cd47, Mcl1* and *Parp1* with or without anti-PD-1 as in Figure 4O, were analyzed by flow cytometry. **(A)** PD-1 MFI on $CD44^+CD8^+$ TIL in treated mice. **(B)** Mean MFI of CD244, CTLA-4, TIM-3, and LAG-3 on $CD44^+CD8^+$ TIL. **(C-D)** Numbers of $CD8^+$ (C) and NK (D) TIL per mg of tumor. **(E)** Percentage of $CD8^+$ TIL (left) and $CD4^+$ TIL (right) producing IFN-γ and TNF-α after stimulation with PMA and ionomycin. In all panels, n=4. Data shown are mean + s.e.m. Statistical test: A-E, one-way ANOVA with Holm-Sidak's multiple comparisons. *p ≤ 0.05, **p ≤0.01, ***p ≤0.001, ****p≤0.0001.

	EpCAM AsiC sequences
EpCAM-UPF2 sense	GCGACUGGUUACCCGGUCG UUU GCGUUAUGUUUGGUGGAAG dTdT
UPF2 antisense	CUUCCACCAAACAUAACGC dTdT
EpCAM-CD47 sense	GCGACUGGUUACCCGGUCG UUU GAUCAUAGCUCUAGCAGAA dTdT
CD47 antisense	UUCUGCUAGAGCUAUGAUC dTdT
EpCAM-PARP1 sense	GCGACUGGUUACCCGGUCG UUU CCAAAGGAAUUCCGAGAAA dTdT
PARP1 antisense	UUUCUCGGAAUUCCUUUGG dTdT
EpCAM-MCL1 sense	GCGACUGGUUACCCGGUCG UUU AAACGAAGGCGAUGUUAAA dTdT
MCL1 antisense	UUUAACAUCGCCUUCGUUU dTdT
EpCAM-APEX1 sense	GCGACUGGUUACCCGGUCG UUU GGUGAUUGUGGCUGAAUUU dTdT
APEX1 antisense	AAAUUCAGCCACAAUCACC dTdT
EpCAM-CD274 sense	GCGACUGGUUACCCGGUCG UUU AGACGUAAGCAGUGUUGAA dTdT
CD274 antisense	UUCAACACUGCUUACGUCU dTdT

Table. S1. EpCAM AsiC sense and antisense strand sequences. The EpCAM aptamer sequence is in red. The UUU linker sequence is in blue.

	qRT-PCR primer sequences
m*Upf2* Fw	TGTTGCAGTCTCTTGCACAGC
m*Upf2* Rev	GGATCAACGTCTCCTCCCACC
m*Parp1* Fw	CCATCGACGTCAACTACGAG
m*Parp1* Rev	GTGCGTGGTAGCATGAGTGT
m*Cd47* Fw	AGGAGAAAAGCCCGTGAAG
m*Cd47* Rev	TGGCAATGGTGAAAGAGGTC
m*Mcl1* Fw	TTGTAAGGACGAAACGGGAC
m*Mcl1* Rev	TCTAGGTCCTGTACGTGGAAG
m*Apex1* Fw	GGGTGATTGTGGCTGAATTTG
m*Apex1* Rev	GCTGTCGGTATTCCAGTCTTAC
m*Cd274* Fw	CTCATTGTAGTGTCCACGGTC
m*Cd274* Rev	ACGATCAGAGGGTTCAACAC
m*Ifna1* Fw	TCTGTGCTTTCCTGATGGTC
m*Ifna1* Rev	GGTTATGAGTCTGAGGAAGGTC
m*Ifna2* Fw	GAGAGAAGAAACACAGCCCC
m*Ifna2* Rev	AGCAAGTTGACTGAGGAAGAC
m*Ifnb1* Fw	CGAGCAGAGATCTTCAGGAAC
m*Ifnb1* Rev	TCACTACCAGTCCCAGAGTC
m*Gapdh* Fw	CCACTCACGGCAAATTCAAC
m*Gapdh* Rev	CTCCACGACATACTCAGCAC
m*Gadd45a* Fw	AGACCCCGGACCTGCACTG
m*Gadd45a* Rev	TTCGGATGCCATCACCGTTC
m*Gadd45a* pre-mRNA Fw	AGACCCCGGACCTGCACTG
m*Gadd45a* pre-mRNA Rev	ACCCACGAGCTTAGACACGC
m*Gadd45b* Fw	GCCAAACTGATGAATGTGGACC
m*Gadd45b* Rev	AGCAGAACGACTGGATCAGG
m*Gadd45b* pre-mRNA Fw	TCTGACGACCCCCTGACACTC
m*Gadd45b* pre-mRNA Rev	ATGCCTGATACCCGGACGATG
m*Cdnk1a* Fw	CAGATCCACAGCGATATCCAG
m*Cdnk1a* Rev	AGAGACAACGGCACACTTTG
m*Cdnk1a* pre-mRNA Fw	TGGCCTTGTCGCTGTCTTGC
mCdnk1a pre-mRNA Rev	TTTCTCCTTCTCTGCTCCTGTCC
m*Nat9* Fw	GGAGTATGAGATGCAGTGTAGC
m*Nat9* Rev	CAAGGTCTGTGAGGAAGAGG
m*Nat9* pre-mRNA Fw	AGATCGAGGTCATGATTGCAG
m*Nat9* pre-mRNA Rev	ACAATCAGCCACCATCCAG

Table. S2. Primer sequences for qRT-PCR. m indicates mouse gene-specific primer; h indicates human gene-specific primer. Fw: forward, Rev: reverse.

Dataset. S1. Differential exon usage (DEU) after *UPF2* knockdown in EpCAM^{hi} MDA-MB-231. Significant changes in exon usage of 222 genes after *UPF2* knockdown. For each gene, log2 fold change of exon expression after *UPF2* knockdown and adjusted p-values are shown.

Dataset. S2. Differential isoform usage (DIU) after *UPF2* knockdown in EpCAM^{hi} MDA-MB-231. Significant changes of isoform usage in 42 genes, including 37 protein-coding genes.

SI References

1. Akbay EA, et al. (2013) Activation of the PD-1 pathway contributes to immune escape in EGFR-driven lung tumors. *Cancer Discovery* 3(12):1355–1363.

2. Zhang Y, et al. (2017) Enhancing CD8+ T Cell Fatty Acid Catabolism within a Metabolically Challenging Tumor Microenvironment Increases the Efficacy of Melanoma Immunotherapy. *Cancer Cell* 32(3):377–391.e9.

3. Klein AM, et al. (2015) Droplet barcoding for single-cell transcriptomics applied to embryonic stem cells. *Cell* 161(5):1187–1201.